

Molecular Engineering of Myoglobin: The Improvement of Oxidation Activity by Replacing Phe-43 with Tryptophan[†]

Shin-ichi Ozaki,^{*,‡} Isao Hara,[§] Toshitaka Matsui,^{||,⊥} and Yoshihito Watanabe^{*,§,||}

Faculty of Education, Yamagata University, Kojirakawa, Yamagata 990-8560, Japan, Department of Structural Molecular Science, The Graduate School for Advanced Studies, Okazaki, Myodaiji 444-8585, Japan, and Institute for Molecular Science, Myodaiji, Okazaki 444-8585, Japan

Received July 7, 2000; Revised Manuscript Received October 10, 2000

ABSTRACT: The F43W and F43W/H64L myoglobin (Mb) mutants have been constructed to investigate effects of an electron rich oxidizable amino acid residue in the heme vicinity on oxidation activities of Mb. The Phe-43 → Trp mutation increases the rate of one-electron oxidation of guaiacol by 3–4-fold; however, the peroxidase activity for F43W/H64L Mb is less than that of the F43W single mutant because the absence of histidine, a general acid–base catalyst, in the distal heme pocket suppresses compound I formation. More than 15-fold improvement versus wild-type Mb in the two-electron oxidation of thioanisole and styrene is observed with the Phe-43 → Trp mutation. Our results indicate that Trp-43 in the mutants enhances both one- and two-electron oxidation activities (i.e., F43W Mb > wild-type Mb and F43W/H64L Mb > H64L Mb). The level of ¹⁸O incorporation from H₂¹⁸O₂ into the epoxide product for the wild type is 31%; however, the values for F43W and F43W/H64L Mb are 75 and 73%, respectively. Thus, Trp-43 in the mutants does not appear to be utilized as a major protein radical site to form a peroxy protein radical in the oxygenation. The enhanced peroxygenase activity might be explained by the increase in the reactivity of compound I. However, the oxidative modification of F43W/H64L Mb in compound I formation with *m*CPBA prevents us from determining the actual reactivity of the catalytic species for the intact protein. The Lys-C achromobacter digestion of the modified F43W/H64L mutant followed by FPLC and mass analysis shows that the Trp-43–Lys-47 fragment gains a mass by 30 Da, which could correspond two oxygen atoms and loss of two protons.

Hemoproteins perform a wide variety of functions in biological systems (1–6). Among them, myoglobin (Mb), a carrier of molecular oxygen (7), is one of the most intensively studied hemoproteins. With the use of multidisciplinary structural and spectroscopic methods, the roles of individual amino acids in regulating ligand affinity (8–13) as well as heme binding have been addressed in terms of biological functions (14–18).

Myoglobin is also utilized as a framework for molecular engineering studies to probe the structure–function relationships of hemoenzymes (19). Careful examination of the location of amino acid residues in the heme vicinity and the peroxide activation mechanism allowed us to rationally design myoglobin mutants transformed into an efficient hemoenzyme by site-directed mutagenesis (20, 21). In the catalytic cycle of heme-containing peroxidases, compound I, a ferryl species (Fe^{IV}=O) paired with either porphyrin

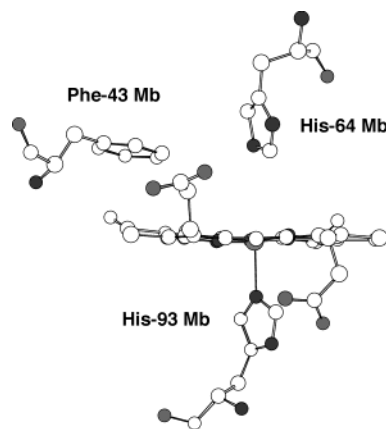


FIGURE 1: Structure of the heme pocket of ferric wild-type sperm whale myoglobin. Heme and some selected amino acid residues, including the proximal histidine (His-93), are shown.

radical cation or protein radical, is essential for oxidation reactions (4). The distal histidine located above the heme iron plays an important role in the formation and reduction of compound I (4, 22). Our previous studies indicate that (a) His-64 in wild-type Mb destabilizes a ferryl porphyrin radical cation and decreases the catalytic activity (22) and (b) the replacement of Phe-43 with a histidine residue, a general acid–base catalyst, accelerates the activation of hydrogen peroxide (Figure 1) (23). We constructed the F43H/H64L double mutant to generate compound I efficiently but

[†] This work was supported by Grant-in-Aid for Scientific Research 10680575 and the Mitsubishi Chemical Corporation Fund (S.-i.O.). This work was also supported by the Scientific Research Priority Area, Molecular Biometallics (Y.W.).

^{*} To whom correspondence should be addressed: Institute for Molecular Science, Myodaiji, Okazaki 444-8585, Japan. Phone: 81-564-55-7430. Fax: 81-564-54-2254. E-mail: yoshi@ims.ac.jp.

[‡] Yamagata University.

[§] The Graduate School for Advanced Studies.

^{||} Institute for Molecular Science.

[⊥] Current address: Institute for Chemical Reaction Science, Tohoku University, Sendai 980-8577, Japan.

limit the leakage of an oxidation equivalent from a ferryl porphyrin radical cation through the distal histidine. As we expected, F43H/H64L Mb exhibits up to 300-fold better oxidation activity with respect to the wild type (23), and compound I of the mutant exhibits an absorption spectrum typical for a ferryl porphyrin radical cation (21). The X-ray crystal structure of F43H/H64L Mb reveals that the distance between N ϵ of the distal histidine and the heme iron is 5.7 Å, which is approximately the same as the distance in horseradish peroxidase (HRP) and is longer than that of wild-type Mb by 1 Å (23, 24). It appears that His-43 in F43H/H64L Mb is not readily oxidized to afford a ferryl species paired with a protein radical (4, 25).

On the other hand, a different approach to promoting enzymatic activity of myoglobin was also reported (26). In wild-type Mb, an electron transfer from His-64 to the porphyrin radical cation initiates the destabilization of compound I (21, 22). The oxidation equivalent temporarily stored at the distal histidine is transmitted through several amino acids, and relatively stable tyrosine or tryptophan radical is eventually formed (27). As a result, one of the oxidation equivalents is completely separated from the heme center, and substrates such as styrene are not oxidized efficiently in the heme pocket (27, 28). Therefore, Wong et al. replaced Phe-43 with a tyrosine residue to retain the second oxidation equivalent as a tyrosine radical in the heme pocket and successfully increased the rate of epoxidation by nearly 30-fold versus wild-type Mb (26). Since a tyrosine is not likely to function as a general acid–base catalyst ($pK_a = 10$), the increase in oxidation activity would be relevant to the enhancement of the reactivity of catalytic species.

The improved enzymatic activity observed with the Phe-43 \rightarrow His (21) and Phe-43 \rightarrow Tyr (26) mutations motivated us to introduce a tryptophan, another electron rich oxidizable residue, at position 43. We have constructed F43W and F43W/H64L Mb and report here that Trp-43 in the mutants increases the one- and two-electron oxidation activity. Furthermore, absorption spectral changes, FPLC, and mass analysis have revealed that the heme pocket of the F43W/H64L mutant is oxidatively modified during the reaction with an oxidant, *m*-chloroperbenzoic acid (*m*CPBA).

EXPERIMENTAL PROCEDURES

Materials. H₂¹⁸O₂ was prepared from ¹⁸O₂ as described by Sawaki and Foote (29), and the ¹⁸O content of the peroxide was determined to be 92% by alkaline epoxidation of menadione (30). All the other chemicals were purchased from Wako or Nakalai Tesque and used without further purification.

Spectroscopy. All spectroscopic measurements were performed in 50 mM sodium phosphate buffer (pH 7.0) unless otherwise indicated. Electronic absorption spectra of purified proteins were recorded on a Shimadzu UV-2400 spectrophotometer. The stopped-flow experiments were performed on a Hi-Tech SF-43 instrument equipped with a MG6000 diode array spectrometer. The Lys-C achromobacter-treated proteins were analyzed on an AKTA FPLC system (Pharmacia), and mass spectra of the fragments were obtained on either a SCIEX instrument (Perkin-Elmer Biosystems, model API 300) for ESI-MS or a Voyager instrument (PerSeptive Biosystems, model DESTRA) for TOF-MS. Both analytical methods provided the same results.

Site-Directed Mutagenesis and Protein Purification. The Phe-43 \rightarrow Trp mutation was introduced by the polymerase chain reaction (PCR)-based method. The expression and purification of the mutants were performed as reported previously (31, 32). Only a single protein band appeared on a SDS–PAGE gel after the purification procedures.

Measurements of One-Electron Oxidation (Peroxidase) Activities. One-electron oxidation activities were measured at 25 °C in 50 mM sodium phosphate buffer (pH 7.0). The typical reaction mixture contained Mb (1 μ M) and guaiacol (2 mM). Steady-state kinetic constants were obtained by measuring the initial rates as the hydrogen peroxide concentration was being varied. The initial rate of guaiacol oxidation was monitored from the increase in absorbance at 470 nm using a molar absorbance coefficient ϵ_{470} of 7.6×10^3 M⁻¹ cm⁻¹ (23). At least two sets of experiments were performed to determine the rates.

Measurements of Two-Electron Oxidation (Peroxxygenase) Activities. The oxidations of thioanisole and styrene were performed at 25 °C in 50 mM sodium phosphate buffer (pH 7.0) (33). The reaction mixture contained Mb (10 μ M for sulfoxidation and 20 μ M for epoxidation), H₂O₂ (1 mM), and either thioanisole (1 mM) or styrene (8.7 mM). For the sulfoxidation assay, acetophenone was added as an internal standard, and the mixture was extracted with dichloromethane for HPLC analysis on a Daicel OD chiral column. The column was eluted with 80% hexane and 20% 2-propanol at a flow rate of 0.5 mL/min, and the effluent was monitored at 254 nm. For the epoxidation assay, 2-phenyl-2-propanol was added as an internal standard, and the dichloromethane extracts were analyzed on a gas chromatograph GC (Shimadzu GC-14B) equipped with a Chiraldex G-TA capillary column. The column temperature was kept at 90 °C for the analysis. The standard curves for sulfoxide and epoxide were prepared for quantitative analysis. The rates were determined from the linear portion of the product versus time plot, and the absolute stereochemistry was determined on the basis of a retention time of the authentic *S* or *R* product.

Determination of Oxygen Source in the Epoxide Product. The wild type or mutants (20 μ M) in 0.5 mL of 50 mM sodium phosphate buffer (pH 7.0) was incubated with styrene (8 mM) and H₂¹⁸O₂ (1 mM) at 25 °C. The dichloromethane extracts of the incubation mixtures were analyzed by GC–MS (Shimadzu GC-17A/GCMS-QP5000) equipped with a Shimadzu CBP1 capillary.

Formation and Reduction of Compound I of F43W/H64L Mb. The reaction of ferric F43W/H64L Mb with *m*CPBA was carried out in 50 mM potassium phosphate buffer (pH 7.4) at 5 °C (21, 22, 33). Spectral changes during compound I formation were recorded on a Hi-Tech SF43 stopped-flow spectrophotometer. The kinetic constants were determined by varying the *m*CPBA concentration under the pseudo-first-order conditions.

The rate of compound I reduction with thioanisole (0.125–1 mM) was measured using a double-mixing rapid scan method in 50 mM potassium phosphate buffer (pH 7.4) at 5 °C. In the first mixing, the ferric F43W/H64L Mb reacted with *m*CPBA (20 equiv with respect to protein) to generate compound I. After the appropriate delay time (0.5 s), thioanisole was added to compound I to monitor spectral

changes. The reaction rate was obtained by fitting the increase in absorbance at 408 nm to a single-exponential function.

Characterization of the Modified F43W/H64L Mutant. F43W/H64L Mb (20 μ M) was treated with 5 equiv of *m*CPBA (100 μ M) for 10 min at 4 °C in 50 mM potassium phosphate buffer (pH 7.4). The mutant treated with *m*CPBA was loaded on a SP-TOYOPEARL 650 M column (2.5 cm \times 30 cm), and the modified protein was separated from excess *m*CPBA and the residual unmodified protein using a linear gradient of 15 mM potassium phosphate (pH 6.0) to 40 mM potassium phosphate (pH 9.0). The typical protein digestion was performed in the presence of myoglobin (600 μ g) and Lys-C achromobacter (40 μ g) in 100 mM Tris-HCl (pH 9.0) containing 2 M urea, and the mixture was incubated at 25 °C for 12 h (34, 35). The digestion was stopped by adding trifluoroacetic acid (TFA) (final concentration of 1%). The digested products were analyzed on a Vydac C-18 reverse phase column eluted at a flow rate of 0.7 mL/min with a gradient of solvent A (0.1% TFA in water) to solvent B (60% acetonitrile and 0.07% TFA in water) over the course of 55 min. The eluent was monitored either at 280 nm for peptides bearing aromatic residues or at 408 nm for heme. Peak fractions were collected and injected directly onto a SCIEX (Perkin-Elmer Biosystems, model API 300) or Voyager instrument (PerSeptive Biosystems, model DESTR) for mass analysis.

RESULTS

Absorption Spectra of F43W and F43W/H64L Mb. The spectra of the ferric, ferrous, and ferrous-CO states of F43W Mb are very similar to the corresponding forms of wild-type Mb (Figure 2) (36). The Soret band at 408 nm with broad bands at 506 and 635 nm indicates a typical hexacoordinated ferric high-spin heme (I). The sixth ligand in the F43W mutant is a water molecule presumably stabilized by His-64 through hydrogen bonding. Since the loss of water ligation in the ferric F43W/H64L mutant causes a Soret shift to 394 nm (9), the novel Trp-43 does not appear to stabilize the heme-bound water. The absorption spectra of the ferrous and ferrous-CO forms of F43W/H64L Mb are essentially identical to those of F43W Mb.

One-Electron Oxidation Activities (Peroxidase Activities) of Wild-Type Mb and Its Mutants. One-electron oxidation of guaiacol by the wild type and its mutants was examined in phosphate buffer (pH 7.0) with H_2O_2 . With increasing concentrations of H_2O_2 , the mutants exhibit a linear increase in activity; therefore, the rate-determining step for the one-electron oxidation process appears to be the reaction of ferric Mb with H_2O_2 . The values in Table 1 are calculated as the slopes of linear portions of the H_2O_2 concentration versus rate plots.

The Phe-43 \rightarrow Trp mutation increases the one-electron oxidation activity by 3–4-fold; i.e., F43W Mb oxidizes guaiacol approximately 4-fold faster than the wild type, and the F43W/H64L mutant exhibits 3-fold better activity than H64L Mb. Since the proton on the indole nitrogen is not exchangeable, Trp-43 cannot function as a general acid–base catalyst like the distal histidine. The deletion of His-64 in F43W Mb decreases the guaiacol oxidation activity by 180-fold. However, the introduction of a tryptophan residue

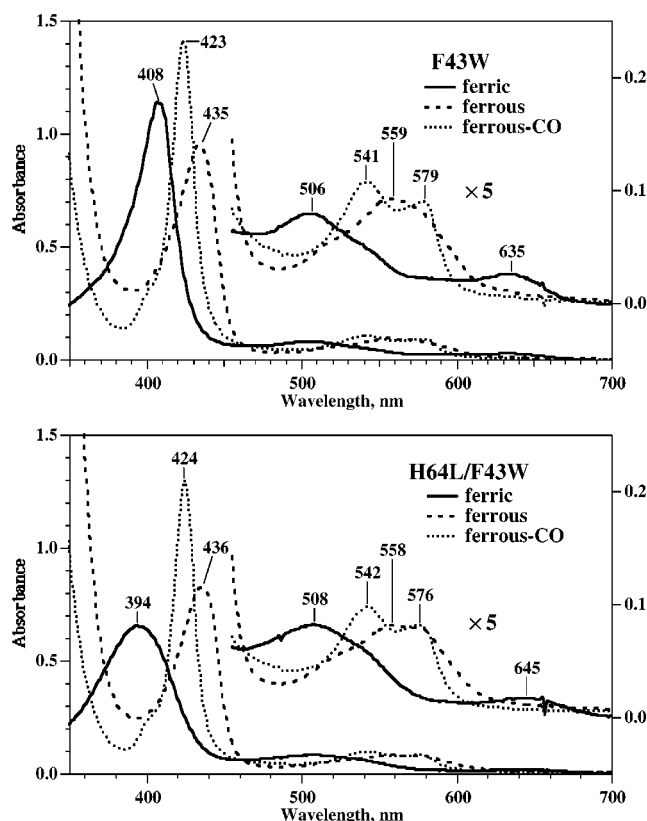


FIGURE 2: Absorption spectra of the ferric (solid line), ferrous (dashed line), and ferrous-CO states (dotted line) for F43W (6 μ M) and F43W/H64L Mb (6 μ M) in 50 mM sodium phosphate buffer (pH 7.0). The visible region starting at 450 nm is magnified, and the absorbance scale is indicated on the right.

Table 1: Guaiacol Oxidation Catalyzed by Wild-Type Mb and Its Mutants

	guaiacol oxidation activity ^a
wild type	32
F43W	140
H64L	0.24
F43W/H64L	0.75

^a All the assays were performed in 50 mM sodium phosphate buffer (pH 7.0). The unit for the oxidation activity is nanomoles of product per nanomole of Mb per minute per millimolar H_2O_2 .

in the active site accelerates the formation of a catalytic species because the rate-determining step for the one-electron oxidation reaction is found to be compound I formation. The indole proton in the active site might increase the affinity for H_2O_2 through hydrogen bonds.

Two-Electron Oxidation Activities (Peroxxygenase Activities) of Wild-Type Mb and Its Mutants. Two-electron oxidations, a ferryl oxygen transfer to thioanisole and styrene, have also been examined (Table 2). F43W Mb exhibits the best two-electron oxidation activity as observed for guaiacol oxidation. The Phe-43 \rightarrow Trp mutation results in the enhancement in oxygenation activities (i.e., F43W Mb > wild-type Mb and F43W/H64L Mb > H64L Mb), and His-64 in myoglobins improves the two-electron oxidation reactions (i.e., F43W Mb > F43W/H64L Mb and wild-type Mb > H64L Mb). The trends here are essentially the same as for one-electron oxidation, but the degree of activity enhancement by the tryptophan mutation is different. Approximately 20-fold improvement in the rate of sulfoxidation

Table 2: Enantioselective Oxidation of Thioanisole and Styrene by Wild-Type, F43W, H64L, and F43W/H64L Mb^a

	thioanisole		styrene	
	rate (min ⁻¹)	% ee	rate (min ⁻¹)	% ee
wild type	0.64	24	0.011	15
F43W	13	30	0.16	48
F43W/H64L	1.9	24	0.11	50
H64L	0.072	27	0.020	34

^a The absolute stereochemistry of the dominant isomer for sulfoxide and epoxide is *R*.

Table 3: Origins of the Oxygen Atom in the Sulfoxide and Epoxide Product

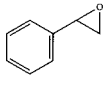
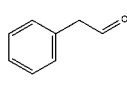
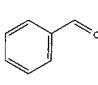
	% ¹⁸ O incorporation from H ₂ ¹⁸ O ₂			
	wild type	F43W	F43W/H64L	H64L
sulfoxidation	87	92	91	89
epoxidation	31	75	73	73

and epoxidation is observed with the replacement of Phe-43 in wild-type Mb with a tryptophan residue. The F43W/H64L mutant oxidizes thioanisole 26-fold faster than H64L Mb. The 15–26-fold increase in two-electron oxidation activity is greater than the enhancement observed for one-electron oxidation of guaiacol (~3–4-fold). The results suggest that the reaction of ferric Mb with H₂O₂ is not the only step controlling the rate of the oxygenation reaction. The reactivity of compound I with thioanisole and styrene might be increased by the replacement of Phe-43 with a tryptophan residue.

The Phe-43 → Trp mutation does not appear to create a specific binding site to produce one of the isomers with high enantioselectivity (Table 2). F43H/H64L Mb (85 and 68% enantiomeric excess for sulfoxidation and epoxidation, respectively) is found to be a better chiral catalyst than the F43W/H64L mutant. Although a clear rationalization for the stereoselectivity in the oxidation system with Mbs has not been provided at the moment, the amino acid at position 43 appears to be one of the important residues for asymmetric oxidations.

To estimate the ratio of a ferryl oxygen transfer versus a peroxy protein radical mechanism, ¹⁸O-labeled H₂O₂ was used to perform the reaction (Table 3). More than 87% ¹⁸O incorporation into the methyl phenyl sulfoxide suggests that a ferryl oxygen transfer mechanism is favored in the sulfoxidation reaction. The low level of ¹⁸O incorporation into the epoxide product for the wild type was explained by a peroxy protein radical mechanism, and Trp-14 eventually bearing one of the oxidation equivalents was recently suggested to be a stable radical site (27). As a result, the oxygen atom of epoxide is derived from molecular oxygen. The level of ¹⁸O incorporation increases from 31 to 73% with the His-64 → Leu mutation presumably because an unoxidizable Leu-64 partially prevents leakage of one of the oxidation equivalents from compound I to form the protein radical. Since the value for F43W/H64L Mb is the same as that of the H64L mutant, Trp-43 does not seem to promote a peroxy protein radical mechanism. In the F43W mutant, the two different oxidation mechanisms could compete; however, 75% incorporation is essentially the same as the values for F43W/H64L and H64L Mb. Thus, compound I of F43W Mb seems to oxidize styrene before losing its

Table 4: Products Formed in the Reaction of Styrene with Wild-Type, F43W, and F43W/H64L Mb^a

			
	styrene oxide	phenylacetaldehyde	benzaldehyde
Wild Type	57 %	25 %	18 %
F43W	34	61	5
F43W/H64L	42	52	6

^a The oxidized product ratios are reported in percent.

oxidation equivalents through His-64. The result might imply the increase in reactivity of compound I by the Phe-43 → Trp mutation in the active site.

Styrene is oxidized not only to styrene oxide but also to benzaldehyde and phenylacetaldehyde (Table 4). Benzaldehyde is produced in the H₂O₂-supported oxidation of styrene by most hemoproteins via an unknown mechanism, but phenylacetaldehyde is formed by a hydrogen rearrangement reaction (37–39). Since the proton transfer to the benzylic carbon would be favored in a polar active site, the ratios of these three products could help us estimate the polarity of the heme pocket. Phenylacetaldehyde accounts for only 6% of the total products for H64L Mb, and the ferric state of the mutant is known to be in the pentacoordinated state, where a water molecule is not bound to the iron (9). The percentages of phenylacetaldehyde are 25% (wild-type Mb), 61% (F43W Mb), and 52% (F43W/H64L Mb), which are greater than the values for H64L Mb. Although the absorption spectrum of F43W/H64L Mb indicates that a water molecule is not coordinated to the heme iron, there might be some water molecules stabilized by Trp-43 (i.e., N–H of the indole moiety) through hydrogen bonding in the heme pocket.

Formation and Reduction of Compound I. The results of two-electron oxidation activities suggest that the Phe-43 → Trp mutation might increase the reactivity of compound I. To examine the implication, we decided to determine the rate of compound I reduction for F43W/H64L Mb in the presence of thioanisole using a stopped-flow apparatus. Compound I can be observed in the His-64 deletion mutants when *m*CPBA is used as an oxidant because the distal histidine lies in a path for the oxidation equivalents to leak out (22). The absence of a general acid catalyst in the mutants can be compensated by the use of *m*CPBA bearing a carboxylate moiety as a good leaving group to achieve the heterolytic cleavage of the oxygen–oxygen bond.

Typical absorption spectral changes upon mixing of the F43W/H64L mutant and *m*CPBA are shown in Figure 3A. Addition of 10–50 equiv of *m*CPBA to F43W/H64L Mb with a Soret maximum at 394 nm first produces a sharp and more intense Soret band at 408 nm. Then, the spectrum changes to a typical compound I spectrum with an approximately 2-fold decrease in the Soret intensity with an intense absorbance around 500–700 nm. The kinetic constant (*k*₁) for the formation of an intermediate (compound X) with a λ_{max} of 408 nm is 1.3 × 10⁵ M⁻¹ s⁻¹ (Figure 3B). The rate of compound I formation is also proportional to the concentration of *m*CPBA, and the kinetic constant (*k*₂) is 1.9 × 10⁴ M⁻¹ s⁻¹ (Figure 3B).

The reduction of F43W/H64L Mb compound I with thioanisole causes an increase in absorbance at 408 nm with

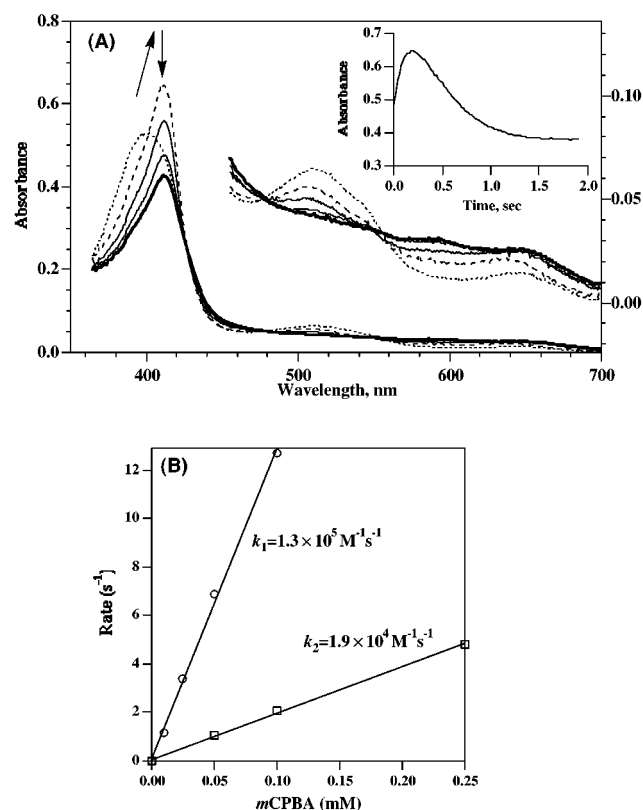


FIGURE 3: (A) Absorption spectral changes of F43W/H64L Mb upon mixing with *m*CPBA. The dotted line and thick line represent spectra of the initial ferric state and compound I, respectively. The dashed line is an intermediate, compound X, observed prior to compound I formation. In the inset are shown the absorbance changes at 408 nm vs time. The visible region starting at 450 nm is magnified, and the absorbance scale is indicated on the right. (B) Plots of *m*CPBA concentration vs the rate of compound X formation or compound I formation. The rate constants (k_1 and k_2) were determined as the slopes.

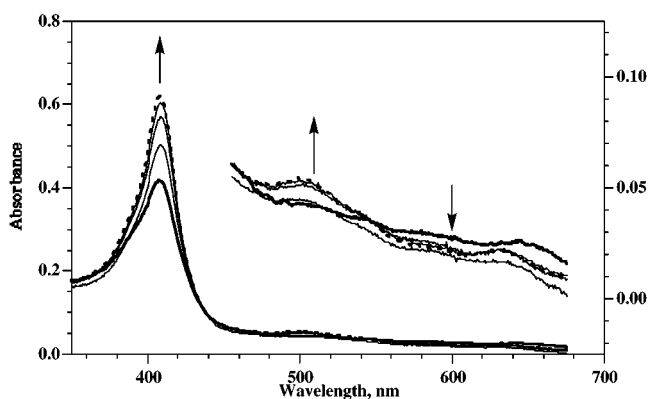
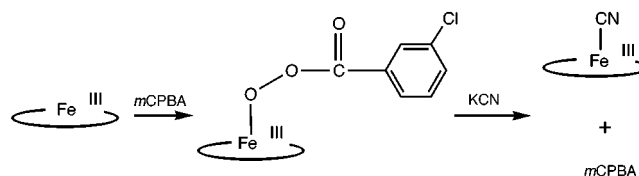


FIGURE 4: Reduction of compound I for F43W/H64L Mb in the presence of thioanisole. Arrows indicate directions of absorbance changes. The thick line indicates compound I immediately after the mixing, and the dashed line represents the ferric state (8 ms after adding thioanisole). The spectra taken every 2 ms are shown. The visible region starting at 450 nm is magnified, and the absorbance scale is indicated on the right.

no shift of the Soret band ($k_3 = 4.5 \times 10^5 \text{ M}^{-1} \text{ s}^{-1}$) (Figure 4). The spectrum after the reduction is essentially the same as that of compound X, and compound I of F43W/H64L Mb has never been reduced to a pentacoordinated ferric form with the Soret band at 394 nm. In compound I formation with *m*CPBA, *m*-chlorobenzoic acid (*m*CBA), which could

Scheme 1



be bound to the ferric heme iron, is produced as a side product. However, mixing the F43W/H64L mutant with *m*CBA does not shift a Soret band from 394 to 408 nm. Therefore, the species with a λ_{max} of 408 nm (compound X) seems to be the hexacoordinated ferric high-spin state heme with a water molecule as the sixth ligand.

Characterization of Compound X. Compound X is generated simultaneously by adding approximately 2 equiv of *m*CPBA to F43W/H64L Mb, and the species is stable enough to be observed and isolated at room temperature. To ascertain features of compound X, several experiments were performed.

We first generated compound X and then added potassium cyanide. If compound X is a heme-*m*CPBA adduct, a ligand exchange occurs to form a cyanide-heme iron complex. It would be possible to titrate the amount of *m*CPBA with potassium iodide (Scheme 1). Upon addition of potassium cyanide, we observed a red shift of the Soret band, which is an indication of cyanide complex formation. However, iodide was not oxidized to triiodide because there was no increase in absorbance at 353 nm for I_3^- .

Since triiodide would react with an amino acid like a tyrosine residue in the protein, we further attempted to quantitate *m*CPBA, if it is released from compound X, with thioanisole. Thioanisole is simultaneously oxidized in the presence of a stoichiometric amount of *m*CPBA, and the sulfoxide product is analyzed by HPLC. In the experiment, an excess of potassium cyanide (20 mM) was added to compound X (20 μM) and cyanide complex formation was confirmed by the absorption spectrum. Then, thioanisole (1 mM) was added to the solution; however, the sulfoxide product was not observed in the dichloromethane extract.

The results suggest that (a) a ligand originally bound to the heme iron in compound X can exchange with cyanide, (b) *m*CPBA is not released from compound X upon addition of potassium cyanide, and (c) compound X does not have oxidation equivalents. Although direct evidence like the crystal structure is necessary to make conclusions about structural features of compound X, our observations imply that compound X does not seem to be a highly reactive heme-*m*CPBA complex. We speculated that chemical modifications of the F43W/H64L mutant by *m*CPBA cause structural changes in the heme pocket. If the oxygenation of the active site residues occurs, a water molecule bound to the heme iron as the sixth ligand could be stabilized through hydrogen bonding interactions. We hypothesize that compound X is in the ferric high-spin state with a water molecule as the distal ligand.

To examine our hypothesis and identify the modification site, we treated F43W/H64L Mb with Lys-C achromobacter, separated the digested products by FPLC, and then determined the molecular masses of the peptide fragments by ESI-MS and TOF-MS. The F43W/H64L mutant yielded four major fragment peaks in the FPLC chart when monitored at

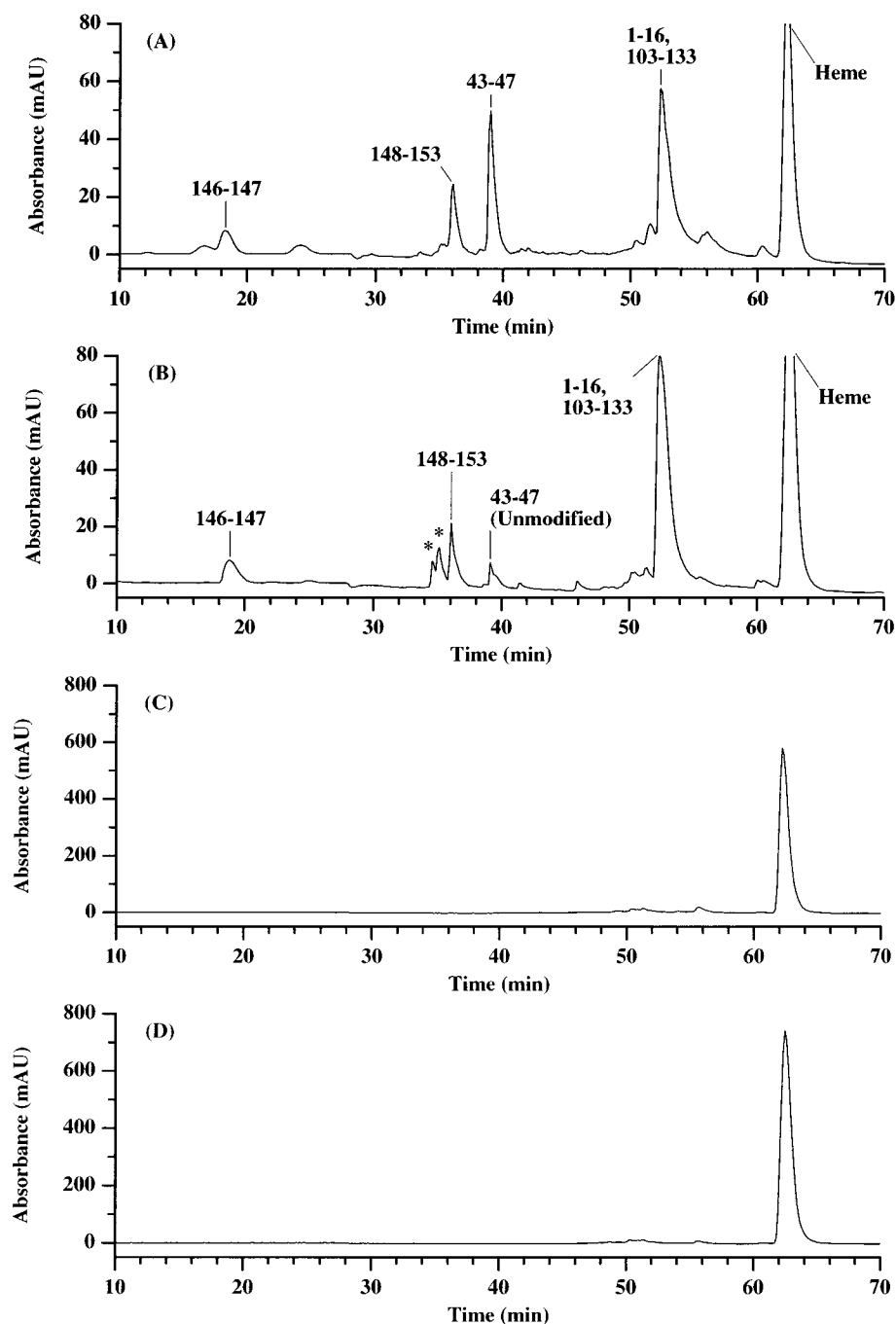


FIGURE 5: FPLC profile of Lys-C achromobacter-treated F43W/H64L Mb (A and C) and Lys-C achromobacter-treated F43W/H64L Mb after reaction with *m*CPBA (B and D). The traces monitored at 280 (A and B) and 408 nm (C and D) are shown.

280 nm, which are assigned to (1) Tyr-146–Lys-147, (2) Glu-148–Gly-153, (3) Trp-43–Lys-47, and (4) a mixture of Val-1–Lys-16 and Tyr-103–Lys-133 peptides in the elution order by mass analysis (Figure 5A). All the fragments bearing aromatic residues were identified in the control experiment. In addition, the heme released from the protein is found to be eluted at 62 min by monitoring at 408 nm (Figure 5C,D).

In the chromatograph of *m*CPBA-treated F43W/H64L Mb, two new peaks indicated with asterisks appear before the Trp-43–Lys-47 peptide (WDRFK) elutes, and the intensity of the peak assigned to the intact WDRFK fragment is diminished (Figure 5B). Both of the new adducts have a mass of 781.4 Da, which is greater than the molecular mass of

the Trp-43–Lys-47 fragment by 30 Da (Figure 6). Furthermore, the MS/MS analysis of the *m*CPBA-treated Trp-43–Lys-47 fragment suggests that Trp-43 is the exact modification site. The results suggest that (1) the reaction of F43W/H64L Mb with *m*CPBA produces two different adducts, (2) the modification site is Trp-43, and (3) the 30 Da increase in mass after the reaction could be associated with the addition of two oxygen atoms and the loss of two protons. The addition of polar oxygen atoms is consistent with the retention times of the modified adducts being shorter than that of the intact Trp-43–Lys-47 fragment. Furthermore, the absorption spectral changes on going from the penta- to hexacoordinated high-spin state upon reaction with *m*CPBA could also be rationalized by the stabilization of a water

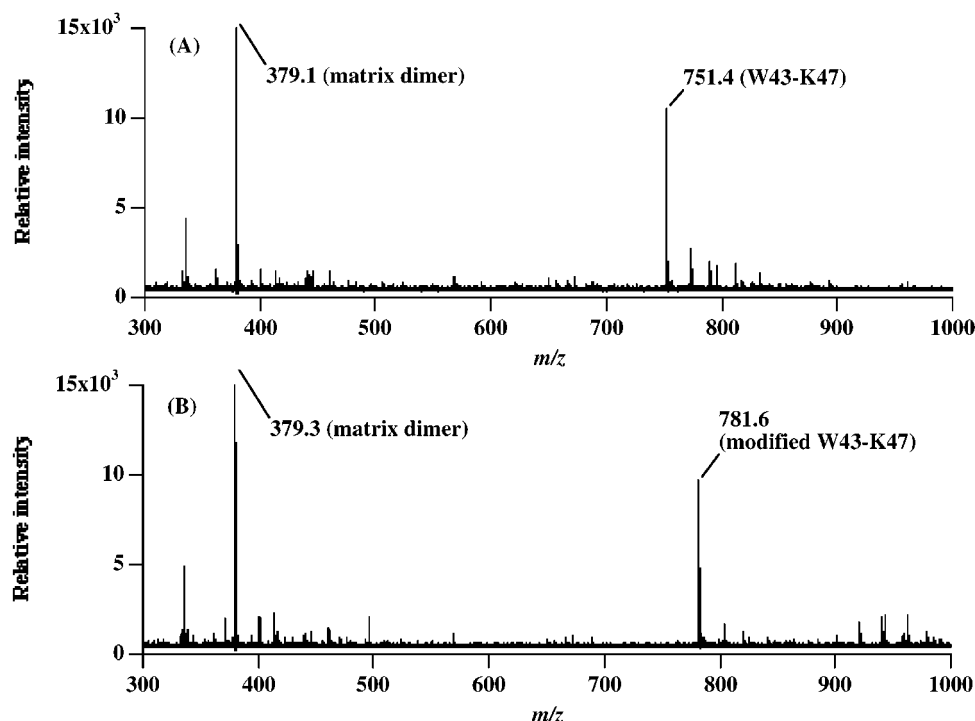


FIGURE 6: TOF-MS spectrum of (A) the Trp-43-Lys-47 fragment and (B) the Trp-43-Lys-47 fragment treated with *m*CPBA.

molecule bound to the heme iron through hydrogen bonding interactions with the oxygenated amino acid residues. Although the autocatalytic hydroxylation at the β -carbon of Trp-171 in lignin peroxidase has recently been reported (40, 41), a similar mechanism may not be applied in the myoglobin mutant. We speculate at the moment that the tryptophylquinone isomers are produced because the absorption spectrum of the modified Trp-43-Lys-47 fragment (λ_{\max} at 397 nm) is similar to those of indolequinone model compounds synthesized previously (42). Further studies on the exact structure of the heme pocket for the modified F43W/H64L mutant as well as the oxygenation mechanism are now underway.

It should be noted that the reaction of F43W/H64L Mb with H_2O_2 does not produce a compound X-like absorption spectrum with a λ_{\max} of 408 nm, and the oxidative modification of the protein is not observed. Thus, compound X appears to be generated only when *m*CPBA is present as an oxidant. More importantly, the modified F43W/H64L mutant does not seem to be involved in the oxidation of guaiacol, thioanisole, and styrene when H_2O_2 is used as an oxidant (Tables 1–3).

DISCUSSION

The results presented here indicate that the replacement of Phe-43 with Trp enhances both one- and two-electron oxidation activities. In the one-electron process, compound I formation is the rate-determining step, and Trp-43 in the active site of the mutants accelerates the reaction of ferric Mb with H_2O_2 (Table 1). The hydrogen bonding interactions through the indole ring as well as the polar heme environment might favor the activation of H_2O_2 to generate compound I efficiently (43). The tryptophan side chain, however, cannot function as a general acid–base catalyst. Therefore, the absence of the distal histidine in the F43W/H64L mutant

suppresses the one-electron oxidation of guaiacol with respect to the wild type.

On the other hand, compound I formation does not seem to be the sole rate-determining step in the two-electron process. The Phe-43 \rightarrow Trp single replacement facilitates the epoxidation and sulfoxidation by 15–25-fold, which is similar to the degree observed for the Phe-43 \rightarrow His and Phe-43 \rightarrow Tyr mutations (21, 26), but the mutation increases the rate of compound I formation by only 3–4-fold (Table 2). Furthermore, the ferryl oxygen transfer process is slower than the one-electron oxidation reaction. The enhanced activity for the tryptophan mutants would not be due to the increase in substrate accessibility because a tryptophan residue is larger than a phenylalanine. To examine if the reactivity of compound I is improved by the Phe-43 \rightarrow Trp mutation, we performed a single-turnover experiment on a stopped-flow apparatus. In the experiment, compound I of F43W/H64L Mb was first generated using *m*CPBA as an oxidant, and then thioanisole was mixed to measure the reduction rate. The rate constant for compound I reduction with thioanisole (k_3) is $4.3 \times 10^5 \text{ M}^{-1} \text{ s}^{-1}$. The value is slightly greater than that for H64L Mb ($k_3 = 3.1 \times 10^5 \text{ M}^{-1} \text{ s}^{-1}$) but does not seem to be large enough to account for the 26-fold enhancement in sulfoxidation activity caused by the Phe-43 \rightarrow Trp/His-64 \rightarrow Leu double mutation.

However, the absorption spectral changes during the reaction of F43W/H64L Mb with *m*CPBA suggest that the pentacoordinated ferric high-spin state is transformed into the hexacoordinated ferric high-spin state (compound X) prior to compound I formation (Figure 3). Characterization of compound X by FPLC and mass analysis reveals that the active site of the F43W/H64L mutant is oxidatively modified. Thus, the rate of compound I reduction determined here is not for the intact but for the modified F43W/H64L mutant. Importantly, such a modification does not seem to occur

during the oxidation of guaiacol, thioanisole, and styrene with H_2O_2 because the absorption spectral changes were not observed. The oxidation activity with H_2O_2 for the intact F43W/H64L mutant might not necessarily reflect the reactivity of compound I for the modified protein.

Although the exact structure of the modified Trp-43–Lys-47 fragment remains to be elucidated, there is no doubt that the substitution of Phe-43 with a tryptophan residue causes the modification of the active site in the presence of *m*CPBA as an oxidant. The tryptophylquinone-like structure we propose here is still no more than speculation, but tryptophan tryptophylquinone (TTQ) is known as a covalently bound cofactor for methylamine dehydrogenase (MADH) (44–46).

In summary, the replacement of Phe-43 with a tryptophan residue enhances one- and two-electron oxidation activities (i.e., F43W Mb > wild-type Mb and F43W/H64L Mb > H64L Mb). Our results support the hypothesis that an electron-rich oxidizable residue at position 43 would improve the catalytic activity. The improved peroxidase activity (i.e., one-electron process) is due to the acceleration in compound I formation. The enhanced peroxygenase activity (i.e., two-electron process) might be explained by the increase in the reactivity of compound I. However, the rationalization remains to be proved because the oxidative modification of F43W/H64L Mb in compound I formation with *m*CPBA prevents us from determining the actual reactivity of the catalytic species for the intact protein. Finally, the combination of FPLC and MS analysis allows us to determine that Trp-43 gains a mass by 30 Da due to the post-translational modification. The further mechanistic studies on the myoglobin's post-translational modification such as the source of oxygen atoms of the modified adducts are awaited.

ACKNOWLEDGMENT

We thank Dr. John Olson (Rice University, Houston, TX) for providing cDNA of sperm whale myoglobin.

REFERENCES

- Antonini, E., and Brunori, M. (1971) *Hemoglobin and Myoglobin in Their Reactions with Ligands*, North-Holland Publishing Co., Amsterdam.
- Ho, C. (1982) *Hemoglobin and Oxygen Binding*, Elsevier, New York.
- Moore, G. R., and Pettigrew, G. W. (1990) *Cytochromes C*, Springer-Verlag, New York.
- Everse, J., Everse, K. E., and Grisham, M. B. (1991) *Peroxidases in Chemistry and Biology*, Vols. I and II, CRC Press, Boca Raton, FL.
- Lippard, S. J., and Berg, J. M. (1994) *Principles of Bioinorganic Chemistry*, University Sciences Books, Mill Valley, CA.
- Ortiz de Montellano, P. R. (1995) *Cytochrome P450*, 2nd ed., Plenum Press, New York.
- Wittenberg, B. A., Wittenberg, J. B., and Caldwell, P. R. B. (1975) *J. Biol. Chem.* 250, 9038–9043.
- Carver, T. E., Rohlf, R. J., Olson, J. S., Gibson, Q. H., Blackmore, R. S., Springer, B. A., and Sligar, S. G. (1990) *J. Biol. Chem.* 265, 3168–3176.
- Quillin, M. L., Arduini, R. M., Olson, J. S., and Phillips, G. N. (1993) *J. Mol. Biol.* 234, 140–155.
- Ikeda-Saito, M., Dou, Y., Yonetani, T., Olson, J. S., Li, T., Regan, R., and Gibson, Q. H. (1993) *J. Biol. Chem.* 268, 6855–6857.
- Sakan, Y., Ogura, T., Kitagawa, T., Fraunfelder, F. A., Mattera, R., and Ikeda-Saito, M. (1993) *Biochemistry* 32, 5815–5824.
- Cameron, A. D., Smerdon, S. J., Wilkinson, A. J., Habash, J., Helliwell, J. R., Li, T., and Olson, J. S. (1993) *Biochemistry* 32, 13061–13070.
- Krzywda, S., Murshudov, G. N., Brzozowski, A. M., Jaskolski, M., Scott, E. E., Klizas, S. A., Gibson, Q. H., Olson, J. S., and Wilkinson, A. J. (1998) *Biochemistry* 37, 15896–15907.
- Hughson, F. M., and Baldwin, R. L. (1989) *Biochemistry* 28, 4415–4422.
- Hargrove, M. S., Singleton, E. W., Quillin, M. L., Ortiz, L. A., Phillips, G. N., Mathews, A. J., and Olson, J. S. (1994) *J. Biol. Chem.* 269, 4207–4214.
- Hargrove, M. S., Krzywda, S., Wilkinson, A. J., Dou, Y., Ikeda-Saito, M., and Olson, J. S. (1994) *Biochemistry* 33, 11767–11775.
- Hargrove, M. S., and Olson, J. S. (1996) *Biochemistry* 35, 11310–11318.
- Kiefhaber, T., and Baldwin, R. L. (1996) *J. Mol. Biol.* 252, 122–132.
- Ozaki, S., Matsui, T., Roach, P. M., and Watanabe, Y. (2000) *Coord. Chem. Rev.* 198, 39–59.
- Ozaki, S., Matsui, T., and Watanabe, Y. (1996) *J. Am. Chem. Soc.* 118, 9784–9785.
- Ozaki, S., Matsui, T., and Watanabe, Y. (1997) *J. Am. Chem. Soc.* 119, 6666–6667.
- Matsui, T., Ozaki, S., and Watanabe, Y. (1997) *J. Biol. Chem.* 272, 32735–32738.
- Matsui, T., Ozaki, S., Liong, E., Phillips, G. N., and Watanabe, Y. (1999) *J. Biol. Chem.* 274, 2838–2844.
- Phillips, G. N. J., Arduini, R. M., Springer, B. A., and Sligar, S. G. (1990) *Proteins: Struct., Funct., Genet.* 7, 358–365.
- Huyett, J. E., Doan, P. E., Gurbel, R., Houseman, A. L. P., Sivaraja, M., Goodin, D. B., and Hoffman, B. M. (1995) *J. Am. Chem. Soc.* 117, 9033–9041.
- Levinger, D. C., Stevenson, J.-A., and Wong, L.-L. (1995) *J. Chem. Soc., Chem. Commun.*, 2305–2306.
- DeGray, J. A., Gunther, M. R., Tschirret-Guth, R., Ortiz de Montellano, P. R., and Mason, R. P. (1997) *J. Biol. Chem.* 272, 2359–2362.
- Catalano, C. E., Choe, Y. S., and Ortiz de Montellano, P. R. (1989) *J. Biol. Chem.* 264, 19534–19541.
- Sawaki, Y., and Foote, S. T. (1979) *J. Am. Chem. Soc.* 101, 6292–6296.
- Ortiz de Montellano, P. R., and Catalano, C. E. (1985) *J. Biol. Chem.* 260, 9265–9271.
- Springer, B. A., and Sligar, S. G. (1987) *Proc. Natl. Acad. Sci. U.S.A.* 84, 8961–8965.
- Springer, B. A., Egeberg, K. D., Sligar, S. G., Rohlf, R. J., Mathews, A. J., and Olson, J. S. (1989) *J. Biol. Chem.* 264, 3057–3060.
- Ozaki, S., Yang, H.-J., Matsui, T., Goto, Y., and Watanabe, Y. (1999) *Tetrahedron: Asymmetry*, 183–192.
- Fenwick, C. W., and English, A. M. (1996) *J. Am. Chem. Soc.* 118, 12236–12237.
- Tschirret-Guth, R. A., Medzihradszky, K. F., and Ortiz de Montellano, P. R. (1998) *J. Am. Chem. Soc.* 120, 7404–7410.
- Takano, T. (1977) *J. Mol. Biol.* 110, 537–568.
- Miller, V. P., DePillis, G. D., Ferrer, J. C., Mauk, A. G., and Ortiz de Montellano, P. R. (1992) *J. Biol. Chem.* 267, 8939–8942.
- Rao, S. I., Wilks, A., and Ortiz de Montellano, P. R. (1993) *J. Biol. Chem.* 268, 803–809.
- Ozaki, S., and Ortiz de Montellano, P. R. (1995) *J. Am. Chem. Soc.* 117, 7056–7064.
- Blodig, W., Doyle, W. A., Smith, A. T., Winterhalter, K., Choinowowski, T., and Piontek, K. (1998) *Biochemistry* 37, 8831–8838.
- Blodig, W., Smith, A. T., Winterhalter, K., and Piontek, K. (1999) *Arch. Biochem. Biophys.* 370, 86–92.
- Moënné-Loccoz, P., Nakamura, N., Itoh, S., Fukuzumi, S., Gorren, A. C. F., Duine, J. A., and Sanders-Loehr, J. (1996) *Biochemistry* 35, 4713–4720.

43. Matsui, T., Ozaki, S., and Watanabe, Y. (1999) *J. Am. Chem. Soc.* **121**, 9952–9957.
44. Chen, L., Mathews, F. S., Davidson, V. L., Huizinga, E. G., Vellieux, F. S., Duine, J. A., and Hol, W. G. J. (1991) *FEBS Lett.* **287**, 163–166.
45. McIntire, W. S., Wemmer, D. E., Chistoserdov, A. E., and Lidstrom, M. E. (1991) *Science* **252**, 817–824.
46. Tanizawa, K. (1995) *J. Biochem.* **118**, 671–678.

BI001579G